

Article

Self-Cleaning Mineral Paint for Application in Architectural Heritage

Sudipto Pal ^{1,*}, Vincenzo Contaldi ², Antonio Licciulli ¹ and Fabio Marzo ¹

¹ Department of Engineering for Innovation, University of Salento, 73100 Lecce, Italy; antonio.licciulli@unisalento.it (A.L.); fabio.marzo@unisalento.it (F.M.)

² Salentec srl, Via dell'Esercito 8, Cavallino, 73020 Lecce, Italy; vincenzo.contaldi@salentec.it

* Correspondence: sudipto.pal@unisalento.it; Tel.: +39-0832-297321

Academic Editor: Enrico Quagliarini

Received: 3 June 2016; Accepted: 13 October 2016; Published: 18 October 2016

Abstract: A mineral silicate paint has been developed for architectural heritage. To enhance durability, any type of organic additive has been avoided. Potassium silicate was the binder agent intended to give strong adherence and durability to stone and concretes. Incorporation of mainly anatase titanium dioxide was intended to act both as a white, bright pigment and as a photocatalyst. Reflectivity analyses on the paint in the visible-to-near infrared wavelength region show high solar heat reflection. The self-cleaning activity of the mineral paint was evaluated by the degradation of organic dyes under solar light irradiation. Anatase titania was effective in decomposing organic and airborne pollutants with the solar radiation. The optical properties and self-cleaning activity were compared with the organic binder-based paints and commercial paints. Developed paints possess high stability: since they contain only inorganic components that do not fade with exposure to solar radiation, photocatalytic self-cleaning capability further enhances such stability.

Keywords: silicate binder; TiO₂ pigment; white paint; solar reflectance; dye degradation; self-cleaning

1. Introduction

There has been high demand for innovative materials for the conservation of architectural heritage and for protecting buildings against the harsh conditions due to increasing environmental pollution [1–3]. Atmospheric pollution and bad air quality, particularly in the urban areas, accelerates the deterioration of the exterior wall surfaces of the buildings. To prevent this, architectural coatings such as liquid pigment suspensions are being developed and designed to protect and decorate houses and buildings [4,5]. Organic and impervious protective coatings can deteriorate prematurely because of their poor lightfastness, therefore worsening the state of the conservation of historical buildings. The architectural coatings industry is continuously searching for new alternatives to improve their products, by reducing costs or improving performance. Because of the reduced VOCs (volatile organic compounds) and less toxicity and odor, waterborne inorganic paints are the greatest choice and the building industries are showing great interest toward developing easy-to-clean and de-polluting surfaces, which can be cleaned by a simple rainfall by using the advancement of nanotechnology [2,6,7]. In this context, photocatalytic paints (containing photo-active titanium dioxide (TiO₂) as a white pigment) could solve the issue thanks to the well-known self-cleaning activity of TiO₂, which could effectively remove inorganic and organic pollutants as well as dirt and stains [8–10].

Silicate mineral potassium or sodium silicate as inorganic binders have several advantages over the polymer binder, such as excellent adhesion to inorganic walls such as those made of stones and ceramic bricks. Silicate paint provides UV resistivity, durability, water vapor permeability, and fire resistance and represents a green sustainable solution. As the silicate paints consist of natural mineral compounds, they are extremely eco-friendly and have no detrimental effect on the environment. Potassium silicate or

water glass, when used as an inorganic binder, reacts with the underlying substrates and creates chemical bonding to the mineral surfaces by silicification (by reacting with the atmospheric carbon dioxide) rather than making a film or coating on the surface when a polymer is used in paint [11,12]. The strong and permanent chemical bonding between the substrate and the paint coating protects the coated surface against the extreme climatic conditions. On the other hand, the photochemically active titanium white pigments combined with organic binder is contradictory due to the adverse effect of photo-degradation of the polymeric binder itself [13,14]. This may lead to the self-deterioration of the coated film under outdoor exposure causing the so-called paint-chalking phenomenon [14,15], thus limiting the use of highly photoactive pigments in waterborne paints. To overcome this problem, either less photoactive pigments such as pure rutile TiO_2 are used or the photoactivity is hindered by coating the TiO_2 particles with a thin layer of SiO_2 or Al_2O_3 . The use of self-cleaning photocatalytic titania additives in paints containing organic binders and additives is controversial, thus limiting their applicability. The use of silicate binder not only prevents the coating from self-degradation but also enhances the photoactivity of the painted surface as the active TiO_2 pigments are more open to the environment due to the porous nature of the coatings [15,16]. It is evidenced from the literature that some previous researchers have studied the effect of alkali silicates as the inorganic binder in paint formulation but this system has not been explored extensively so far, especially in photoactive self-cleaning coatings [11,15–17]. Either different types of mineral binders have been investigated [11,17] or commercial silicate paints have been used in paint formulation [15,16]. In any case even when mineral paints are used, some organic components are generally employed [15]. In this work we report the formulation of highly reflective photocatalytic paint containing potassium silicate as the inorganic binder and TiO_2 as the photoactive agent. All paint components, i.e., binders, flowing agents, thickeners, are purely inorganic to provide longer life and to avoid photocatalytic degradation of the organic fraction. The paint showed high reflectivity in the visible-to-NIR (near infrared) region, maintaining its high self-cleaning activity. The paint surface has been studied in terms of microstructural analysis and the self-cleaning activity was evaluated by organic dye degradation on the paint surface under solar light irradiation.

2. Materials and Methods

2.1. Paint Formulation and Coating Deposition

Two water-based paints, one with organic binder and the other with inorganic binder were prepared by using Aeroxide P25 Titanium dioxide (TiO_2) (Evonik Corporation, Hanau, Germany; average particle size 25 nm, BET surface area $\sim 50 \text{ m}^2/\text{g}$, 80% anatase and 20% rutile) as the photocatalytic pigment material as well as solar reflector and CaCO_3 as filler and extender. The paint with organic binder is denoted as “resin paint” whereas the inorganic binder is named “silicate paint” and maintained throughout this article. In case of resin paint, two type of binders, mainly Silres BS45 (silicone resin emulsions, Wacker Chemie AG, München, Germany), and ENCOR 2423 (styrene acrylic emulsion, Arkema, Milan, Italy) were used as received. For the silicate paint, Betolin K35, a potassium silicate solution with 35 wt % of solid content ($\text{SiO}_2/\text{K}_2\text{O}$ weight ratio 2.2, Wöllner GmbH, Ludwigshafen, Germany) was used as the inorganic binder. Stabilizers and rheological additives were used to get the optimum viscosity and stability of the paint. A certain amount of colloidal silica (Ludox SK, Grace GmbH & Co. KG, Worms, Germany; containing 25 wt % of silica SiO_2 nanoparticles) was also used as an additive to the potassium silicate binder to enhance the adherence property of the paint. In both the paints, a fixed amount of TiO_2 (15 wt %) and CaCO_3 (30 wt %) were maintained. The amount of organic counterpart (20 wt %) in resin paint (50% Silres BS45 and 50% ENCOR 2423) was replaced by potassium silicate binder. Additionally in case of silicate paint, 75% of the water used in resin paint was replaced by water suspension of colloidal silica. Composition of the paints are given in Table 1. The ingredients were mixed by a high speed mechanical stirrer according to the order as reported in Table 1 unless they are mixed well and allowed overnight to remove the bubbles that were formed during the mixing. To compare the experimental data obtained from the synthesized paints, a commercial photocatalytic

paint was purchased from Barozzi Vernici Srl (Revere, Italy), and named as commercial paint throughout the manuscript. The paints were applied on fired bricks and standard black and white paper for optical characterization by doctor blade method [18]. In each case, the wet thickness value was set to $\sim 400 \mu\text{m}$ so that after drying it becomes to $\sim 200 \mu\text{m}$ which is the standard procedure to obtain a paint coating by the doctor blade method used in the paint industry. After applying paint, the coated surfaces were left at room temperature for drying (in both cases complete drying was observed after 12 h at $\sim 25 \text{ }^\circ\text{C}$).

Table 1. Composition of the resin paint and the silicate paint.

Ingredients (wt %)	Resin Paint	Silicate Paint
Water	31	8
Colloidal silica	–	18
Organic modifiers	4	–
ENCOR 2423	10	–
Silres BS45	10	–
TiO ₂	15	15
CaCO ₃	30	30
Potassium silicate	–	26
Stabilizer	–	1.5
Aluminosilicate	–	1.5
Total	100	100

2.2. Characterization

The properties of organic binders and other inorganic species were investigated by observing the vibrational modes in a FTIR Spectrometer with Attenuated Total Reflectance (ATR) sampling accessory (Spectrum One, Perkin Elmer, Shelton, CT, USA). Infrared spectra were collected at frequency range of $4000\text{--}400 \text{ cm}^{-1}$ with the resolution of 4 cm^{-1} by accumulating 32 scans. Surface morphology of the paints was investigated by a Field Emission Scanning Electron Microscope (FESEM) (Zeiss Sigma VP, Carl Zeiss Microscopy GmbH, Jena, Germany). Solar reflectance was evaluated by measuring the diffuse reflectance spectra in the wavelength range of $200\text{--}2500 \text{ nm}$ using a Cary 5000 UV-Vis-NIR spectrophotometer (Agilent Technologies, Inc., Santa Clara, CA, USA) equipped with a 150 mm PTFE-coated integrating sphere. To exclude interferences with the substrate, the spectra were measured with the paint applied on black paper. The total solar reflectance (TSR) was calculated according to the ASTM E903 standard (weighted ordinates method), by integrating the spectral reflectance $\rho(\lambda_i)$ over the solar spectral irradiance distribution, E_λ , as follows:

$$\text{TSR} = \frac{(\sum_{i=1}^n \rho(\lambda_i) E_{\lambda_i}) \Delta\lambda_i}{\sum_{i=1}^n E_{\lambda_i} \Delta\lambda_i} \quad (1)$$

where n is the number of wavelengths for which E_λ is known. Near IR to far IR spectra (2.5 to $25 \mu\text{m}$) were measured using a Spectrum 2000 FTIR instrument (Perkin Elmer, Shelton, CT, USA) equipped with a diffuse gold coated integrating sphere.

2.3. Evaluation of Self-Cleaning Activity

Photoactivity of the paints was evaluated by photocatalytic degradation of organic pollutants (dye molecules). It was evaluated by observing the decomposition of two types of organic dyes, rhodamine B and methylene blue in aqueous solution under a solar light irradiation. A fixed amount ($200 \mu\text{L}$) of each dye solution ($20 \mu\text{M}$) was dropped on to the painted surface so that a circular spot is formed and left overnight under the dark to reach the adsorption equilibrium. Then they were placed under a 300 W solar lamp (Sanolux, Radium Lampenwerk, Wipperfurth, Germany; Irradiance 13.6 W/m^2 at $315\text{--}400 \text{ nm}$ and 41.4 W/m^2 at $380\text{--}700 \text{ nm}$ wavelength) in an air-cooled photo-reactor keeping a distance of 30 cm from the lamp to the paint surface. The photocatalytic degradation of dyes was observed by measuring the absorption spectra of the dyes at a certain time intervals on the paint surfaces by diffuse reflectance method.

2.4. Evaluation of Water Condensation

The water condensation experiment was carried out to evaluate the ability of the coatings to absorb the water that is condensed on the coated surface from the surrounding humid air according to the test method developed by Nordtest (NT Poly 170). The paints were applied on the outer surface of an open cylindrical stainless steel container with conical bottom followed by drying at room temperature until a constant weight is obtained. Then the container is filled with a mixture of ice and water so that the steel surface reaches to 0 °C. Then they are left in a controlled climatic chamber at 23 °C and 50% of relative humidity for water condensation and absorption until water starts to drip from the bottom tips. The amount of absorbed water is determined by calculating the weight gain of the paint after removing the ice/water and wiping out any remaining water inside the container. Then they are dried in ambient to achieve the constant weight and the procedure was repeated to re-determine the absorption capacity. This process simulates the cycles of absorption and release by evaporation during the temperature change in the environment.

3. Results and Discussion

Three kinds of paint (i) resin, (ii) silicate and (iii) commercial, were applied on the standard black and white paper for optical and morphological characterizations. Figure 1 shows the FESEM surface morphology of the organic and inorganic coatings. From the micrographs it is clearly visible that the silicate paint surface is more rough and porous in nature whereas the resin paint shows a more compact surface morphology. This feature further enhances the brightness of the paint, as it is evidenced from the optical measurement. If we look in to the high resolution images (Figure 1b,d), agglomerated particles that are expected to be nanocrystalline TiO₂ particles are clearly visible in the case of silicate paint whereas a similar feature is not distinguished in the resin paint. Thus, the organic binder hides the visibility of TiO₂ particles in the resin paint whereas the presence of colloidal silica along with the silicate mineral binder helps to form the porous structure. This feature confirms more the porous structure and breathing ability of the buildings coated with silicate paint that comes from the porosity. The cross-sectional images are shown in Figure 2 where the coated surfaces could be clearly distinguished from the substrate. The silicate paint shows a coating thickness of ~230 μm whereas for the resin paint it is ~220 μm (inset of Figure 2). Also, the cross-section investigation confirms that the silicate paint is more porous than the resin paint, as it is expected.

To investigate the nature of the inorganic and organic binders of the paints, ATR-FTIR spectroscopy was employed and showed in Figure 3. A weak and broad band around 3400 cm⁻¹ is observed due to the hydroxyl stretching vibration [14,19]. In the case of silicate paint a strong and relatively broad peak centered at 1078 cm⁻¹ is observed which has a different appearance than the absorption band of the resin paint at a similar frequency region. This band can be assigned to the asymmetric stretching of Si–O–Si [20] superimposed with the Si–O–K band vibrations originating from the silica nanoparticle suspension and the potassium silicate binder, respectively [21]. In both the paints some common features are observed that can be identified as the calcium carbonate (CaCO₃) extender, which shows strong absorption around 1400–1427 cm⁻¹ (asymmetric stretching of CO₃²⁻) and 872 cm⁻¹ (out-of-plane bending of CO₃²⁻) and a relatively weak peak at 712 cm⁻¹ due to CO₃²⁻ in-plane bending [22–24]. Another common feature is the presence of a broad absorption band at 500–700 cm⁻¹, which is arising from the Ti–O–Ti stretching vibration of TiO₂ pigments [19,20,24].

Apart from these common bands, there are significant appearances of other absorption bands in the case of resin paint that are arising from the organic binders. A bunch of distinct peaks at 2962, 2928, and a shoulder at 2870 cm⁻¹ could be assigned to the C–H stretching vibration of the acrylic group whereas a strong peak at 1733 cm⁻¹ can be identified as the carbonyl stretching (C=O) vibration, which is the characteristic absorption band of styrene-modified acrylic resin [23]. The other peaks at 1027–1116 cm⁻¹ could be attributed to the C–O–C asymmetric stretching overlapped with the Si–O–Si asymmetric stretching vibration, and a sharp peak at 1270 cm⁻¹ due to Si–CH₃ symmetric stretching

could confirm the presence of silicon resin emulsion. The absence of several characteristic bands due to the active organic groups in the case of silicate paint represents its pure inorganic nature.

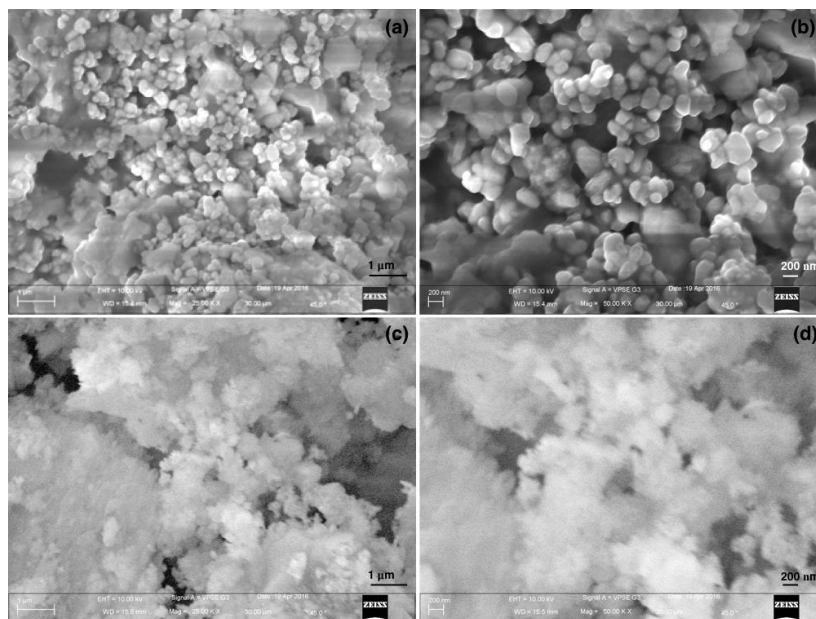


Figure 1. Field Emission Scanning Electron Microscope (FESEM) micrographs of (a,b) silicate paint and (c,d) resin paint surfaces.

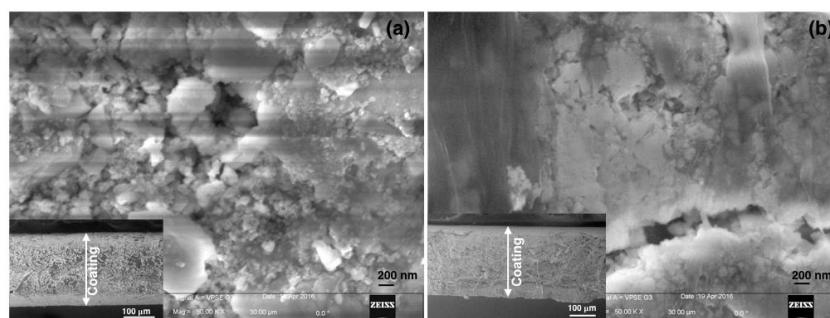


Figure 2. Cross-sectional FESEM micrographs of (a) silicate paint and (b) resin paint. The inset shows the cross-section at a lower magnification.

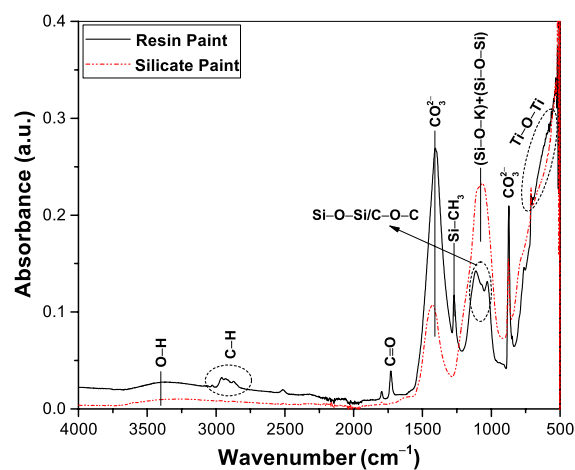


Figure 3. FTIR spectra of the resin and silicate paints. Different vibrational bands are shown in the graph.

The whiteness, the hiding power and the ability to reflect solar radiation were evaluated by measuring the reflectance spectra of the painted surfaces. Figure 4 shows the diffuse reflectance spectra of resin paint, silicate paint and commercial paint for comparison. The spectra were measured in the wavelength range of 200–2500 nm, i.e., the full solar spectrum. The silicate paint shows a maximum reflectance of ~95% at the visible wavelength region where the solar radiation intensity is at the maximum. The resin paint shows about 4% less reflectivity than the silicate paint whereas the commercial paint shows a lower reflectivity, around 88%. The total solar reflection (TSR) values calculated by taking the ASTM G173 solar irradiation as the reference spectrum on different paint surfaces are listed in Table 2. The individual average values of solar reflectance in UV, visible and NIR wavelength regions are also presented. As the superiority of a white paint is determined by the TSR value, silicate paint shows a better performance than the other two paints. Another important characteristic of a paint surface is the emissivity at the thermal IR region that contributes to the ability of a building to keep cooler or warmer. A higher emissivity value indicates the greater rate of releasing the absorbed heat to the atmosphere, thus keeping a building much cooler. The emissivity of a surface can be calculated directly from the reflectance spectra at the thermal IR wavelength region and is shown in Figure 5 as performed on the three painted surfaces. The total emissivity of each paint calculated from the reflection spectra in Figure 5 along with the Solar Reflectance Index (SRI) values are reported in Table 2. The SRI is a measure of the roof's ability to reject solar heat, as shown by a small temperature rise. It is defined so that a standard black (reflectance 0.05, emittance 0.90) is 0 and a standard white (reflectance 0.80, emittance 0.90) is 100.

A higher measured solar reflectance index (SRI) than standard white clearly evidences the coolest material. The silicate paint shows a higher SRI value compared to the other two paints. By considering the TSR, emissivity and SRI values, it is noticed that the silicate paint performs much better than the resin paint and the commercial paints.

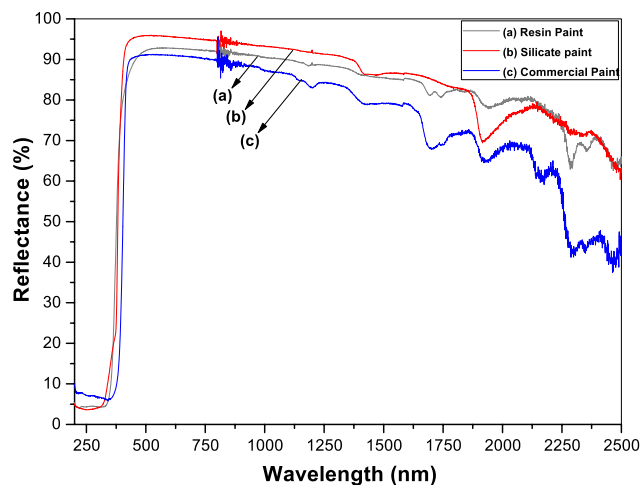


Figure 4. UV-Visible-NIR diffuse reflectance spectra of (a) resin paint, (b) silicate paint and (c) commercial paint.

Table 2. Total solar reflectance (TSR) along with the average reflectivity at three different wavelength regions of the solar spectrum and thermal emittance of three paints.

Samples	Wavelength Range (nm) Reflectivity				Emissivity	Solar Reflectance Index (SRI)
	TSR	UV (300–380 nm)	Visible (380–700 nm)	NIR (700–2500 nm)		
Silicate Paint	91.0	16.7	94.6	91.2	0.91	115.0
Resin Paint	88.2	20.2	90.9	88.9	0.88	110.7
Commercial Paint	84.1	7.4	87.9	84.3	0.89	105.0

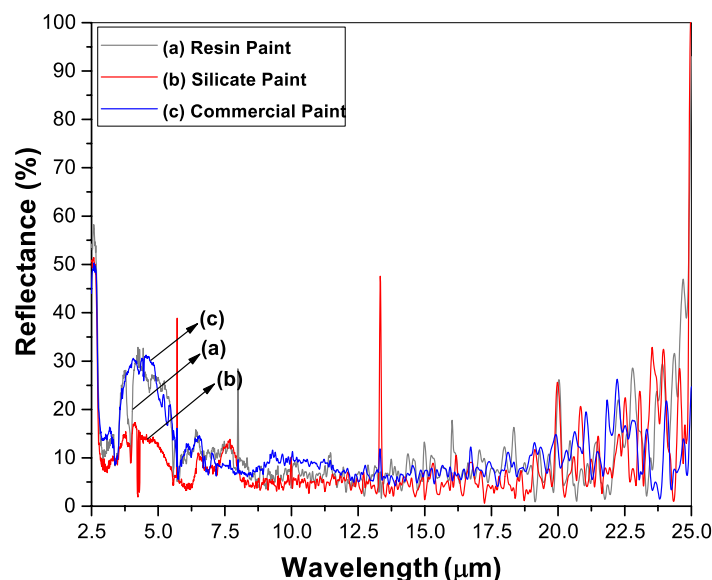


Figure 5. Thermal IR spectra of (a) resin paint, (b) silicate paint and (c) commercial paint.

The self-cleaning activity on the paint was evaluated by the photocatalytic degradation of organic dyes under solar irradiation. Figures 6 and 7 show the pictures of rhodamine B and methylene blue dye droplets on three kinds of paint surfaces as a function of the solar light exposure along with the photocatalytic degradation kinetics. The reaction rate constants were calculated from the plot of C/C_0 with the solar light irradiation time (t) assuming the first-order rate law $[-\ln(C/C_0) = Kt]$, where K is the rate constant [19] and are summarized in Table 3. The silicate paint showed 7 times higher efficiency than the resin and commercial paints in the case of rhodamine B dye and 4–6 times higher efficiency for methylene blue. It is noticeable that the color intensity of the initial (time 0 min) dye droplets on the silicate paint surface (in both cases) looks lighter compared to the other paint surfaces. This is attributed to the porosity-driven hydrophilic surface that causes the droplets to quickly spread over and inside the silicate paint surface. For the other two paints, the surfaces show hydrophobicity due to the presence of silicon and acrylic resins that keep the droplets on the surface and concentrate the dye with solvent evaporation. It is seen from the figures that with increasing the solar light exposure, the color intensity of the dye droplets also decreases, indicating photodegradation of the dye molecules on the paint surfaces. However, the degradation rate is much faster on the silicate paint surface whereas the other two paints show a very poor performance (Table 3). After 30 min of exposure the silicate paint shows almost complete degradation of the dyes which confirms its higher photodegradation efficiency, thus enhancing the self-cleaning activity.

The evaluation of the water condensation experiment in terms of the water absorption capacity on the coated surfaces is reported in Table 4. Data presented are the average of three consecutive measurements. The silicate paint shows 29.7 wt % of water absorption on its surface whereas the commercial paint shows a lower absorption capacity of 13.8 wt %. These can be explained by the porous nature of the silicate paint coating as seen by FESEM measurements. In addition, the time of the first dripping has been measured. The first drip occurred after 58 min in the case of the silicate paint, whereas it was 23 min in the case of the commercial paint. The delay of the first dripping indicates that most of the absorbed water remains inside the coated surface, thus not allowing the formation of droplets on the surface which causes the formation of fungal growth. These data confirm the anti-condensation properties of the paint surfaces. Therefore, the combination effect of photo-induced hydrophilicity, organic pollutant degradation and anticondensation properties make the silicate paint a superior candidate as a self-cleaning paint especially for exterior wall surfaces.

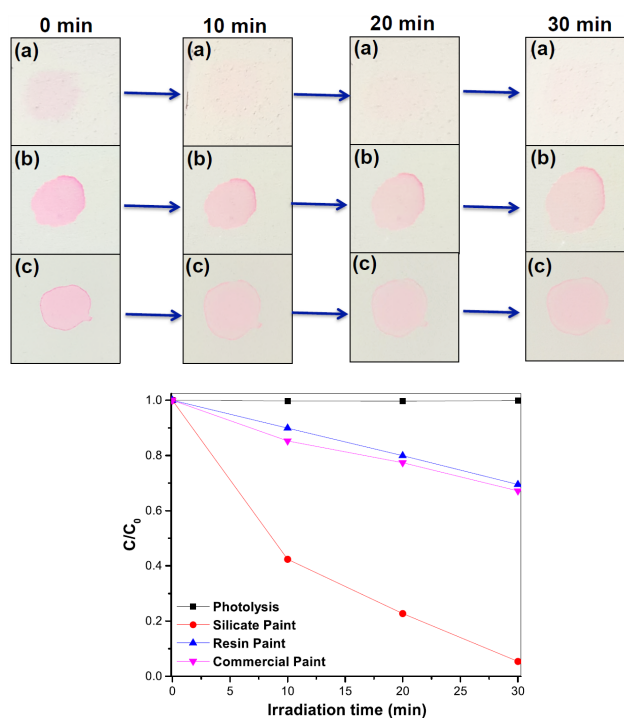


Figure 6. Photodegradation of rhodamine B (RhB) dye aqueous solution (20 μM) performed on (a) silicate paint, (b) resin paint and (c) commercial paint with solar light irradiation time (min). C_0 and C are the initial concentration (at exposure time = 0) and concentration of RhB dyes with solar light irradiation, respectively.

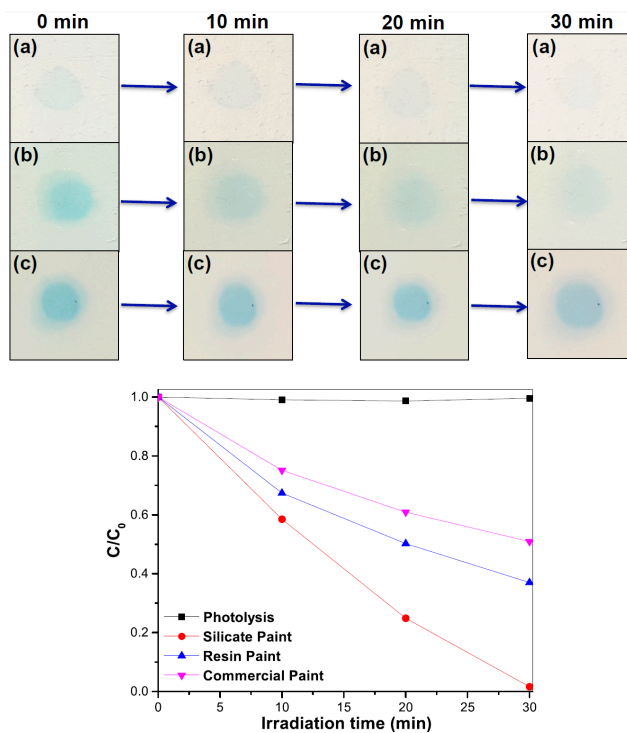


Figure 7. Photodegradation of methylene blue (MB) dye aqueous solution (20 μM) performed on (a) silicate paint, (b) resin paint and (c) commercial paint with solar light irradiation time (min). C_0 and C are the initial concentration (at exposure time = 0) and concentration of MB dyes with solar light irradiation, respectively.

Table 3. Photocatalytic reaction rate constant of rhodamine B and methylene blue dyes performed on different paint surfaces.

Paints	Rhodamine B		Methylene Blue	
	K (min^{-1}) ^a	SD ^b	K (min^{-1}) ^a	SD ^b
Silicate paint	0.093	0.4×10^{-3}	0.132	1.1×10^{-3}
Resin Paint	0.012	2.2×10^{-3}	0.032	2.5×10^{-3}
Commercial Paint	0.013	0.7×10^{-3}	0.022	1.3×10^{-3}

^a Reaction rate constant; ^b Standard deviation.

Table 4. Water condensation and absorption by the painted surface.

Paints	Absorption (wt %) ^a	Dripping Time (min) ^b
Silicate	29.7	58
Commercial	13.8	10

^a Water absorption capacity for a wet coating of 500 g/m²; ^b Time to occur the first dripping in the climatic chamber.

4. Conclusions

An inorganic white paint with high solar and heat reflectivity and self-cleaning activity has been developed and compared with polymeric binder paints. Different properties have been carefully evaluated. The inorganic binder is a mixture of potassium silicate and colloidal silica. The silicate mixture consolidates through a polycondensation reaction while drying in air and forms a strong matrix. This inorganic matrix replaces the conventional organic binders in the photoactive paint formulation, as there is no possibility of self-degradation by the paint itself. The inorganic binder not only enhances the stability of the coating system but also enhances the solar light reflectivity and emissivity that helps to keep the buildings cooler and improve the brightness and aesthetic appearance. Moreover, high efficiency toward organic pollutant degradation makes the silicate paint a great choice as the pollutants that would accumulate on the paint surface could be effectively eliminated by photodegradation under the sunlight. This could help the buildings to remain clean for several years. Self-cleaning and high durability are key features which can be profitably used in architectural heritage. Further investigations will be carried out to evaluate the durability and possibility to improve the self-cleaning and other beneficial properties.

Acknowledgments: The research work has been performed under the framework of the project EFFEDIL. Salentec srl (Lecce, Italy) is thankfully acknowledged for providing the commercial paint and the doctor blade coating facility.

Author Contributions: S. Pal and A. Licciulli conceived and designed the experiments; S. Pal. performed the experiments; V. Contaldi analyzed and discussed optical properties of the paints; F. Marzo performed the microstructural analysis; S. Pal wrote the paper.

Conflicts of Interest: The authors declare no conflict of interest.

References

1. Quagliarini, E.; Bondioli, F.; Goffredo, G.B.; Licciulli, A.; Munafò, P. Smart surfaces for architectural heritage: Preliminary results about the application of TiO₂-based coatings on travertine. *J. Cult. Herit.* **2012**, *13*, 204–209. [[CrossRef](#)]
2. Quagliarini, E.; Bondioli, F.; Goffredo, G.B.; Licciulli, A.; Munafò, P. Self-cleaning materials on architectural heritage: Compatibility of photo-induced hydrophilicity of TiO₂ coatings on stone surfaces. *J. Cult. Herit.* **2013**, *14*, 1–7. [[CrossRef](#)]
3. Goffredo, G.B.; Munafò, P. Preservation of historical stone surfaces by TiO₂ nanocoatings. *Coatings* **2015**, *5*, 222–231. [[CrossRef](#)]

4. Candelaria, P.R.A.; Owens, A.J. Prediction of architectural coating performance using titanium dioxide characterization applying artificial neural networks. *J. Coat. Technol. Res.* **2010**, *7*, 431–440. [[CrossRef](#)]
5. Guo, M.-Z.; Ling, T.-C.; Poon, C.-S. Nano-TiO₂-based architectural mortar for NO removal and bacteria inactivation: Influence of coating and weathering conditions. *Cem. Concr Com.* **2013**, *36*, 101–108. [[CrossRef](#)]
6. Licciulli, A.; Calia, A.; Lettieri, M.; Diso, D.; Masieri, M.; Franza, S.; Amadelli, R.; Casarano, G. Photocatalytic TiO₂ coatings on limestone. *J. Sol-Gel Sci. Technol.* **2011**, *60*, 437–444. [[CrossRef](#)]
7. Munafò, P.; Quagliarini, E.; Goffredo, G.B.; Bondioli, F.; Licciulli, A. Durability of nano-engineered TiO₂ self-cleaning treatments on limestone. *Constr. Build. Mater.* **2014**, *65*, 218–231. [[CrossRef](#)]
8. Chen, J.; Poon, C. Photocatalytic construction and building materials: From fundamentals to applications. *Build. Environ.* **2009**, *44*, 1899–1906. [[CrossRef](#)]
9. Amrhein, K.; Stephan, D. Principles and test methods for the determination of the activity of photocatalytic materials and their application to modified building materials. *Photochem. Photobiol. Sci.* **2011**, *10*, 338–342. [[CrossRef](#)] [[PubMed](#)]
10. Franzoni, E.; Fregni, A.; Gabrielli, R.; Graziani, G.; Sassoni, E. Compatibility of photocatalytic TiO₂-based finishing for renders in architectural restoration: A preliminary study. *Build. Environ.* **2014**, *80*, 125–135. [[CrossRef](#)]
11. Parashar, G.; Bajpayee, M.; Kamani, P.K. Water-borne, non-toxic, high-performance inorganic silicate coatings. *Surf. Coat. Int. B.* **2003**, *86*, 209–216. [[CrossRef](#)]
12. Wilson, A.D.; Nicholson, J.; Prosser, H. *Waterborne Coatings*; Springer: Heidelberg, The Netherlands, 1991; Volume 3, p. 157.
13. Diebold, U. The surface science of titanium dioxide. *Surf. Sci. Rep.* **2003**, *48*, 53–229. [[CrossRef](#)]
14. Wojciechowski, K.; Zukowska, G.Z.; Korczagin, I.; Malanowski, P. Effect of TiO₂ on UV stability of polymeric binder films used in waterborne facade paints. *Prog. Org. Coat.* **2015**, *85*, 123–130. [[CrossRef](#)]
15. Tryba, B.; Wrobel, R.J.; Homa, P.; Morawski, A.W. Improvement of photocatalytic activity of silicate paints by removal of K₂SO₄. *Atmos. Environ.* **2015**, *115*, 47–52. [[CrossRef](#)]
16. Krishnan, P.; Zhang, M.-H.; Cheng, Y.; Riang, D.T.; Yu, L.E. Photocatalytic degradation of SO₂ using TiO₂-containing silicate as a building coating material. *Constr. Build. Mater.* **2013**, *43*, 197–202. [[CrossRef](#)]
17. Gettwert, G.; Rieber, W.; Bonarius, J. One-component silicate binder systems for coating. *Surf. Coat. Int.* **1998**, *81*, 596–603. [[CrossRef](#)]
18. Aegerter, M.A.; Menning, M. *Sol-Gel Technologies for Glass Producers and Users*; Springer: Boston, MA, USA, 2004; pp. 89–92.
19. Pal, S.; Laera, A.M.; Licciulli, A.; Catalano, M.; Taurino, A. Biphasic TiO₂ microspheres with enhanced photocatalytic activity. *Ind. Eng. Chem. Res.* **2014**, *53*, 7931–7938. [[CrossRef](#)]
20. Sanosh, K.P.; Pal, S.; Haq, E.U.; Licciulli, A. Nanocrystalline TiO₂-diatomite composite catalysts: Effect of crystallization on the photocatalytic degradation of rhodamine B. *Appl. Catal. A* **2014**, *485*, 157–162.
21. Osswald, J.; Fehr, K.T. FTIR spectroscopic study on liquid silica solutions and nanoscale particle size determination. *J. Mater. Sci.* **2006**, *41*, 1335–1339. [[CrossRef](#)]
22. Miller, F.L.; Wilkins, C.H. Infrared spectra and characteristics frequencies of inorganic ions. *Anal. Chem.* **1956**, *24*, 1253–1294. [[CrossRef](#)]
23. Germinario, G.; Dorothé van der Werf, I.; Sabbatini, L. Chemical characterisation of spray paints by a multi-analytical (Py/GC-MS, FTIR, μ -Raman) approach. *Microchem. J.* **2016**, *124*, 929–939. [[CrossRef](#)]
24. Di Crescenzo, M.M.; Zendri, E.; Rosi, F.; Miliiani, C. A preliminary FTIR-based exploration of the surfactant phase separation process in contemporary mural paintings. *e-Preserv. Sci.* **2013**, *10*, 10–18.

